Deep Mining 2024 – P Andrieux & D Cumming-Potvin (eds)

doi:10.36487/ACG_repo/2465_16

# Evaluation of alternative mining sequences with consideration of barrier pillar placement at LKAB Kiirunavaara mine

**Theofanis Rentzelos [a,*], Joel Andersson [a], Jonny Sjöberg [a], Linda Jonsson [b], Christina Dahnér [b], Robert Swindell [a], Zsolt Kulcsar [b]**

[a] *ITASCA, Sweden*

[b] *LKAB, Sweden*

## Abstract

*In May 2020 the largest mining-induced seismic event in Sweden to date occurred at the LKAB mine in Kiruna. The event caused significant damage along several hundreds of metres of drifts in the mine in the area known as block 22. Following the event, LKAB permanently stopped the production in the affected area, leaving in place a permanent barrier pillar splitting the Kiirunavaara Mine into a north and south mine.*

*The dimensions of the barrier pillar were determined in a previous study to be about 600 m wide and 350 m high. Preliminary placement was based on minimising ore loss but a more precise adjustment with respect to local geology and rock mechanical aspects remains. Moreover, the current mining sequence must be adjusted with considerations of the barrier pillar for continued mining down to the 1365 m level. A previous study has shown that mining sequences with a more pronounced V-shape (the so-called chevron sequence) can provide more favourable rock mechanical conditions.*

*The scope of this work involved investigating the interaction of alternative mining sequences with the barrier pillar in its preliminary location as well as identifying the optimal sequence from a rock mechanical perspective. Several possible sequences were examined in a 3D mine-scale numerical model in which detailed lithological units and geological structures have been included. Production has been simulated on a quarterly basis in a model without 'coupled flow'. The identified sequence was then analysed in a coupled flow model for verification and further analyses of the influence from the sequence on the barrier pillar as well as the surrounding rock and important mining infrastructure. The model results will be used by the mine in the decision-making process for the transition to a long-term sustainable mining sequence.*

**Keywords:** *sublevel caving, numerical modelling, mine seismicity, FLAC3D-MassFlow*

## 1 Introduction

The Kiirunavaara Mine is the largest underground iron ore mine in the world. The mine is in the north of Sweden and is owned and operated by the Luossavaara-Kiirunavaara AB (LKAB) mining company. The orebody is approximately 4 km long, with a varied width of between about 80 m to 200 m. The mine has an annual production of about 28 Mt via the sublevel caving (SLC) mining method and the deepest extraction point is around 1,000 m from the ground surface. The mine's main haulage level is located at the 1,365 m level (approximately 1,100 m below ground surface). The mine is divided into production blocks. Each production block has a width of approximately 400 m and the block designations are based on the relative block centroid Y-coordinate along the mine's strike.

[*] Corresponding author. Email address: fanis@itasca.se

As in many other deep hard rock mines, large magnitude seismic events are a concern which rises in severity as the mining progresses. In 2020 the largest mining-induced seismic event in Sweden (MW4.2) to date occurred in BL22, causing significant damage to mine infrastructure over a large volume (Svartsjaern et al. 2022). After the consideration of several options regarding the resumption of mining in the affected area, the company decided to permanently stop production in the area and to leave in place a permanent barrier pillar.

The dimensions for the barrier pillar were determined in a previous study (Svartsjaern et al. 2023). The analysis performed indicated a minimum pillar width (along the orebody strike) of 600 m, considering both static stability and seismic potential. The pillar's height extends between the 1,022 m to 1,365 m mining levels. Preliminary pillar placement was chosen by LKAB to minimise potential ore loss, however, the exact location of the pillar and adjustments to its geometry with respect to local geology and rock mechanical considerations remains.

The allocation of the pillar requires revision of the current life of mine plan (LOMP). In the updated LOMP the existing mining sequence is adjusted with consideration of the pillar, but also to achieve the most favourable mining conditions possible, from a rock mechanical perspective, for continued mining down to level 1,365 m.

Previous studies have shown that alternative chevron sequences, with their pronounced V-shape, can offer more favourable rock mechanics behaviour. In this work several chevron mining sequences were analysed numerically and were compared with the mine's currently used sequence. The results showed that a chevron sequence, particularly a double-front moderately steep one, can reduce stress footprints on the mining levels as well as mitigate shear movements when mining through large structures. The implementation of a chevron sequence will, however, result in a more rapid downward advancement compared to previous LOMP's, necessitating faster development of mine infrastructure and transportation plans for material mined below the main level.

# 2 Methodology

The methodology used involved two separate stages. In the first stage, six mining sequences were examined using a numerical model that aimed to identify the most advantageous design considering rock mechanics. A numerical model at a mine-scale was used but without coupled flow. Caving was conceptually simulated by removing rock in the ore and hanging wall above mined areas, which was then replaced with material having parameters corresponding to caving material (Villegas & Nordlund 2008). Infrastructure was not explicitly modelled.

The models were evaluated for stresses, state (plasticity) and the potential for sliding along geological structures. A qualitative estimation of seismic potential was performed by comparing model values with static seismic indicators and limits such as estimated tangential stress, yielding and strength-stress ratio (SSR). The influence on infrastructure was indirectly assessed based on the affected rock mass. The most advantageous mining sequence was identified with respect to rock mechanics, mine planning and practical feasibility. This was done in collaboration with LKAB. In addition, alternative locations and the geometry of the barrier pillar were investigated to find a more optimised design with respect to rock mechanics considerations. The details of this work are not reported below as the paper is more focused on evaluation of mining sequences.

In the second stage the selected sequence and optimal barrier pillar location were further analysed using a coupled MassFlow-FLAC3D model. The coupled model was employed to account for hanging wall caving more accurately. Similarly to the first stage, results were evaluated by analysing the stress state, material yielding and potential for sliding along structures. The second part of the study focused on evaluating the effect of mining with the selected mining sequence on the barrier pillar and the main mining level (at 1,365 m).

# 3 Evaluation of mining sequences

## 3.1 Alternative mining sequences

A total of six different production sequences were examined (Figure 1). Mining was simulated on a quarterly basis to obtain reasonable resolution in the results, especially in terms of stress redistribution. The sequences were developed in consultation with LKAB to develop realistic chevron sequences as follows:

- Base case — current SLC mining sequence
- Steep chevron (A.1) — a chevron sequence with a constant 30° angle and tip towards pillar
- Flattening chevron (B.1) — a chevron sequence with a constant 30° angle and tip towards pillar but flattening after reaching level 1365
- Flat chevron (C.1) — a relatively flatter chevron sequence with ½ mining block (200 m) per sublevel height (28.5 m) and six months advance
- Steep two-front chevron (A.2) — a chevron sequence with a constant 30° angle and two fronts on each side of the pillar
- Flattening two-front chevron (B.2) — a chevron sequence with a constant 30° angle and two fronts on each side of the pillar, with the chevron flattening after reaching level 1365.

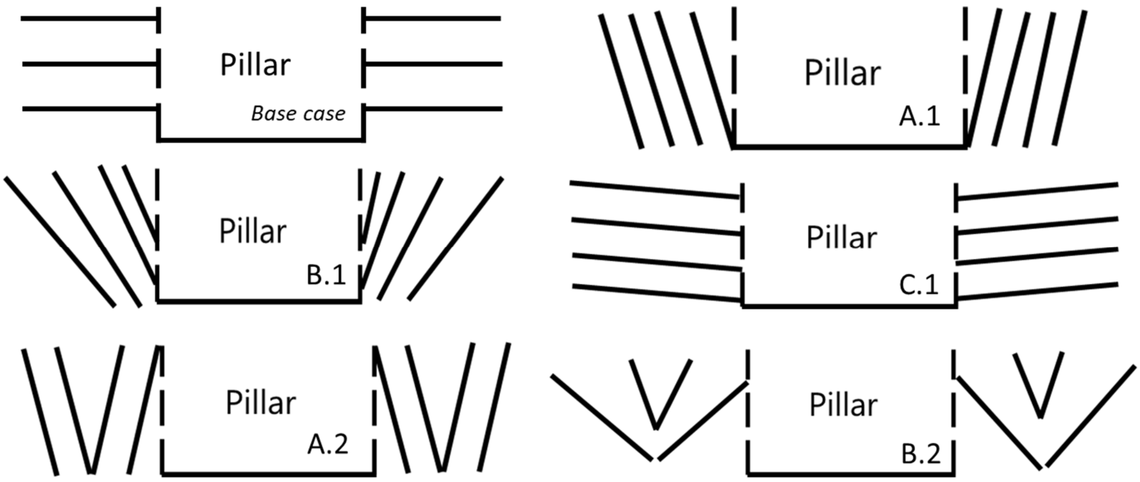


**Figure 1 Schematic Illustration of the analysed mining sequences**

## 3.2 Geology and mechanical properties

The main geological model constitutes the orebody boundary (ore), two diabase dykes (DB), clay alterations (clay) and porphyry dykes (DP), as well as the footwall (syenite porphyries and granite) and the hanging wall (quartz porphyries) (Figure 2). Apart from the main lithological units, the numerical models also included several identified geological structures (Figure 3). These geological structures have been divided into three different types based on their interpreted behaviour in the field.

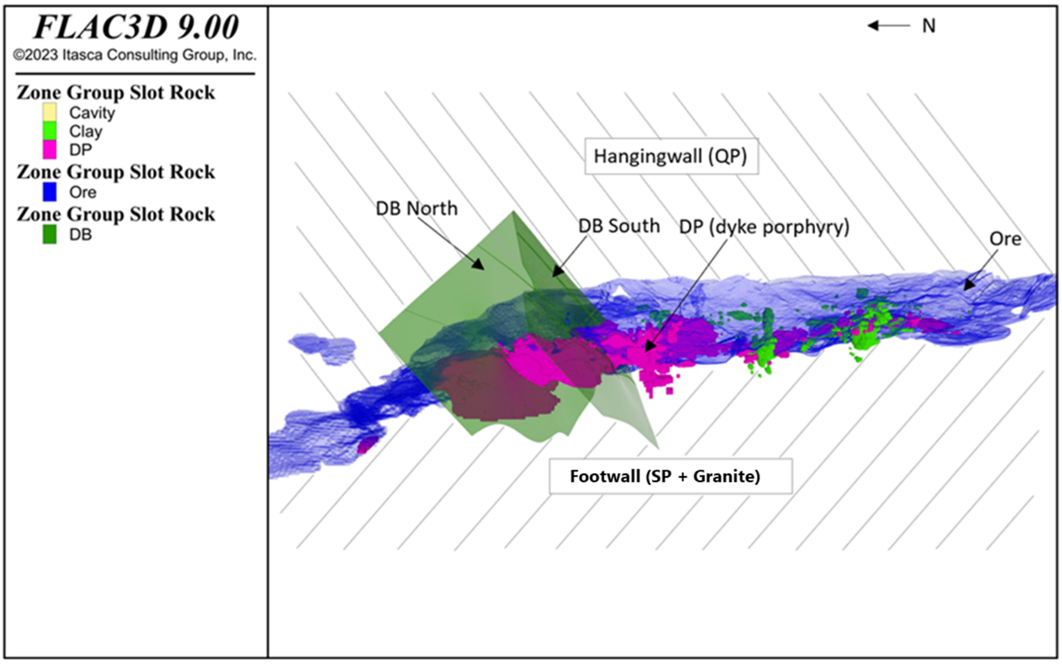


**Figure 2** Illustration of modelled lithological units

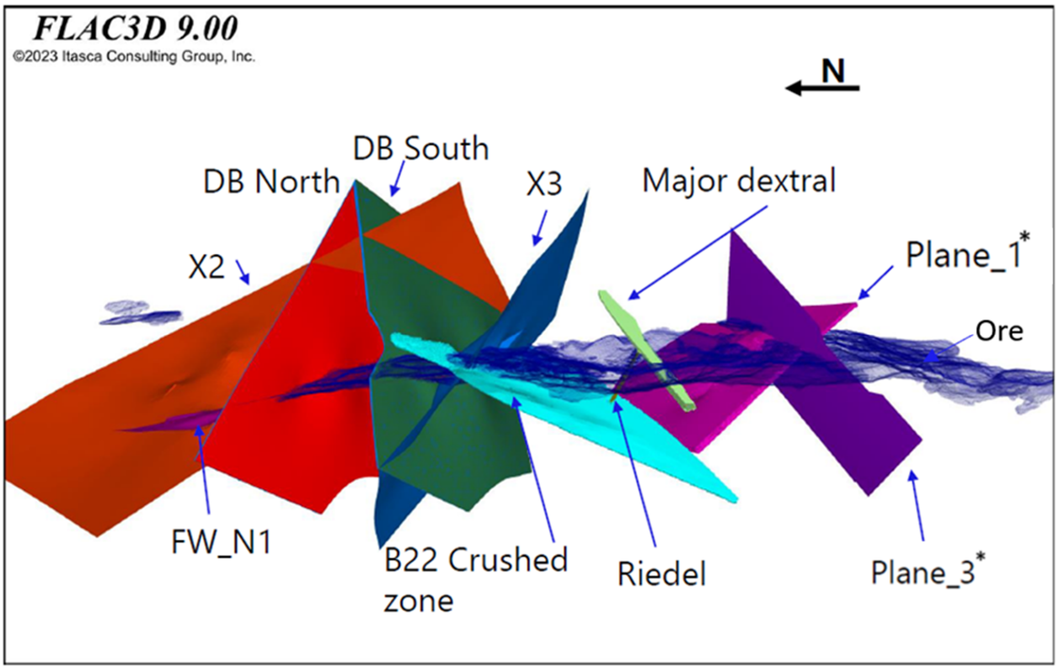


**Figure 3** Identified significant geological structures in the model volume. Structures marked with * were included only in the coupled flow analysis

The B22 crushed zone, Major dextral and Plane_1 were interpreted as weakness zones and modelled as volumes with reduced (lower strength and stiffness) mechanical properties. The structures X2, X3, FW_N1, Riedel and Plane_3 were interpreted as different types of faults with the potential to slip and were included in the model as 'interfaces' (or slip planes). The two DB (DB north and DB south) were included as separate rock units. The contact surfaces between the these and the adjoining country rock were, however, modelled as slip planes.

All geological units, with the exception of clay-altered zones and weakness zones, were assumed to have brittle behaviour and modelled with the strain softening constitutive model IMASS (Itasca Constitutive Model for Advance Strain Softening) (Ghazvinian et al. 2020), with mechanical properties according to Table 1. These properties were based on previously calibrated numerical models for the Kiirunavaara Mine. Both the clay-altered and the weakness zones generally have a more ductile behaviour and were therefore modelled as frictional Mohr–Coulomb materials with mechanical properties according to Table 2. The mechanical properties of the slip planes are summarised in Table 3.

**Table 1 Mechanical properties for units modelled as Itasca Constitutive Model for Advance Strain Softening materials**

| Property | Ore | Footwall (SP + granite) | Hanging wall (QP) | Porphyry dykes (DP) | Diabase dykes (DB) |
|---|---|---|---|---|---|
| Uniaxial compressive strength (MPa) | 183 | 180 | 150 | 320 | 175 |
| Geological strength index | 67 | 76 | 66 | 81 | 44 |
| Young's modulus (GPa) | 60 | 65 | 65 | 65 | 65 |
| $m_i$ | 17 | 20 | 18 | 20 | 15 |
| Poisson's ratio | 0.25 | 0.25 | 0.25 | 0.25 | 0.25 |
| Density (kg/m$^3$) | 4,600 | 2,800 | 2,800 | 2,800 | 2,800 |
| Dilation angle (°) | 10 | 10 | 10 | 10 | 10 |

**Table 2 Mechanical properties for units modelled as Mohr–Coulomb materials**

| Property | Clay | B22 Crushed zone, Major dextral, Plane_3 | Cave and blasted rock |
|---|---|---|---|
| Density (kg/m$^3$) | 2,000 | 2,800/4,600 (i) | 2,000 |
| Young's modulus (GPa) | 0.01 | 1.7 | 0.2 |
| Poisson's ratio | 0.25 | 0.25 | 0.28 |
| Cohesion (MPa) | 0.20 | 3.5 | – |
| Friction angle (°) | 3.5 | 24 | 43 |
| Tensile strength (MPa) | 0 | 0.025 | – |
| Dilation angle (°) | 0 | 10 | – |

(i) Hanging wall/footwall or ore

**Table 3 Mechanical properties for slip planes (Malmgren & Nordlund 2008)**

| Property | X2, X3, FW_N1, Riedel, Plane_1, Diabase contact planes |
|---|---|
| Normal stiffness (GPa/m) | 110 |
| Shear stiffness (GPa/m) | 9 |
| Cohesion (MPa) | 0 |
| Friction angle (°) | 30 |
| Tensile strength (MPa) | 0 |

## 3.3 Model set-up

The FLAC3D (Itasca Consulting Group 2023a) model was built using an 'oct-tree' hybrid mesh in which the mesh is composed of hexahedral zones arranged in structured cubic patterns. The outer dimensions of the model were set to 10,400 × 5,150 × 2,400 m to minimise any potential boundary effects. The cubic hexahedral elements have an edge size of 7 m inside and around the different geological units (except the footwall and hanging wall). The mesh size is then gradually increased to the outmost part of the mesh, where the element size was set to 128 m. The mesh size in different parts of the model is shown in Figure 4. All model boundaries were fixed in their respective normal direction except the top boundary, which was left free to simulate a free ground surface.

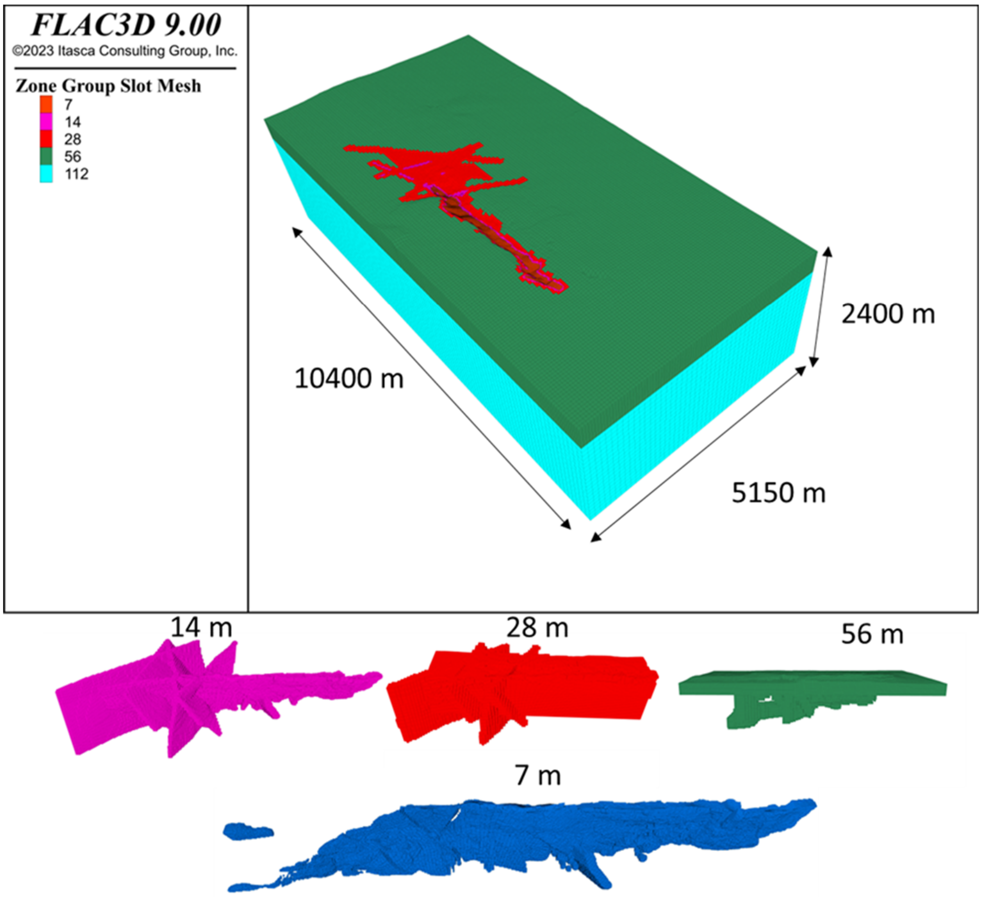


**Figure 4 Model size and gradation**

The initial stress state (prior to initial equilibrium) was based on the stress measurement compilation by Sandström (2003). Compressive stresses are denoted as negative. Initial stresses on mining levels below 215 m were applied as follows, assuming zero stresses at the ground surface of the hanging wall at z = –200 m, with z decreasing towards the depth:

$$\sigma_H = 7.4 + 0.037z,\ \sigma_h = 5.6 + 0.028\ z,\ \sigma_v = 5.8 + 0.029z \quad (1)$$

where:

$\sigma_H$ = major horizontal stress (most compressive) in MPa, orientated semi-perpendicular to the ore strike (east–west).

$\sigma_h$ = minor horizontal stress (least compressive) in MPa, orientated semi-parallel to the ore strike (north–south).

$\sigma_v$ = vertical stress in MPa.

Above the 215 m (z = –215) level, gravitational stresses were assumed for topological features such as the footwall peak. Compressive stresses are negative, displacements are positive when directed along a positive coordinate axis, normal strains are positive for extension and volumetric strain is positive for volume increase.

The structures identified as slip planes are the four planar geological structures (X2, X3 and FW_N1), Riedel and the lithological unit diabase (where the contacts to the host rock can slip). These were all simulated as continuous discrete planes without any thickness where the mesh encompassing them is as an irregular hexahedral mesh which follows the fluctuation of the structures (Figure 5). The irregular hexahedral mesh volumes are attached to the surrounding structures' hexahedral mesh. The two weakness zones (B22 crushed zone and Major dextral) are treated as the other geological units, i.e. with a structured cubic mesh having a zone size of 7 m.

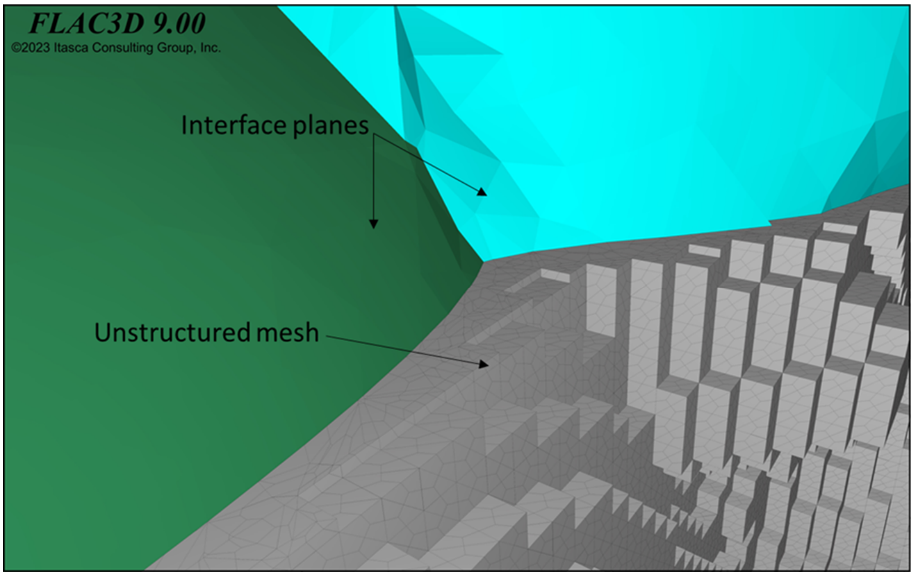


**Figure 5 Example of interface planes and encompassing unstructured mesh**

## 3.4 Results

### *3.4.1 Chevron angle*

The results of the different mining sequences investigated showed significantly different stress redistribution patterns between the steeper and the flattened chevron sequences. For a steep chevron sequence (sequences A.1, B.1, A.2 and B.2) the major principal stress redistributes around the excavation fronts, creating a high stress concentration locally at the most advanced excavation front of each level. For a flatter sequence (base case and sequence C.1) the stress redistributes mainly below the mined levels. This can lead to a larger footprint of high stresses on two to three of the levels below the current mining level (Figure 6).

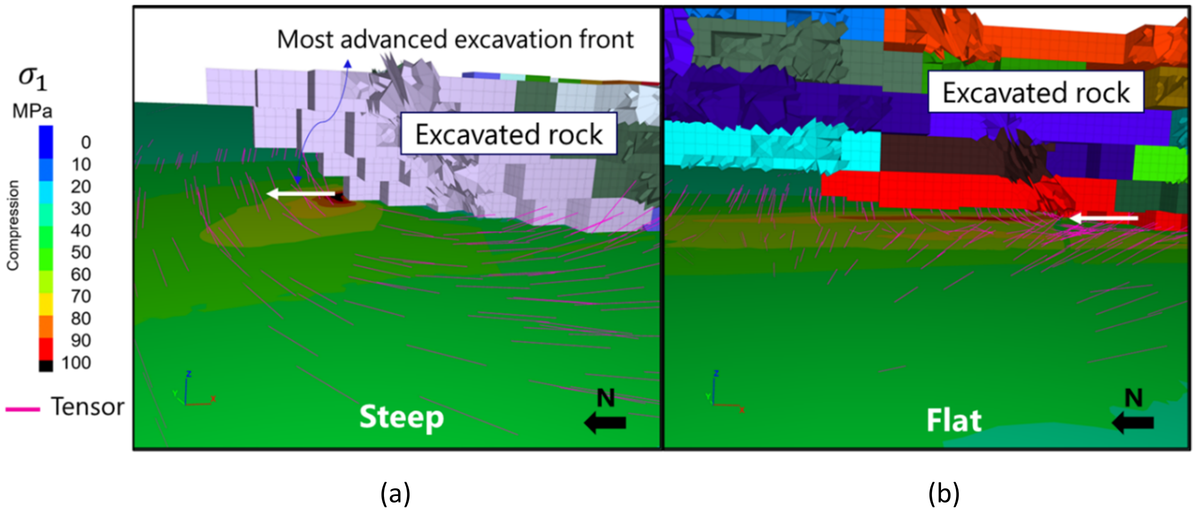


**Figure 6 Redistribution of major principal stress in (a) a steep and (b) a flat chevron sequence**

A comparison of the SSR shows that with a steeper chevron sequence, every new level opens in a relatively unaffected stress environment since the influence of the levels above is limited (Figure 7). The same behaviour also continues during mining of the level, since the influence of the already mined levels is always larger for the flattened sequences. This influence is particularly evident around large weakness zones (e.g. BL22 crush zone, Major dextral), which can undergo extensive yielding to create possibly worse conditions when they are mined through.

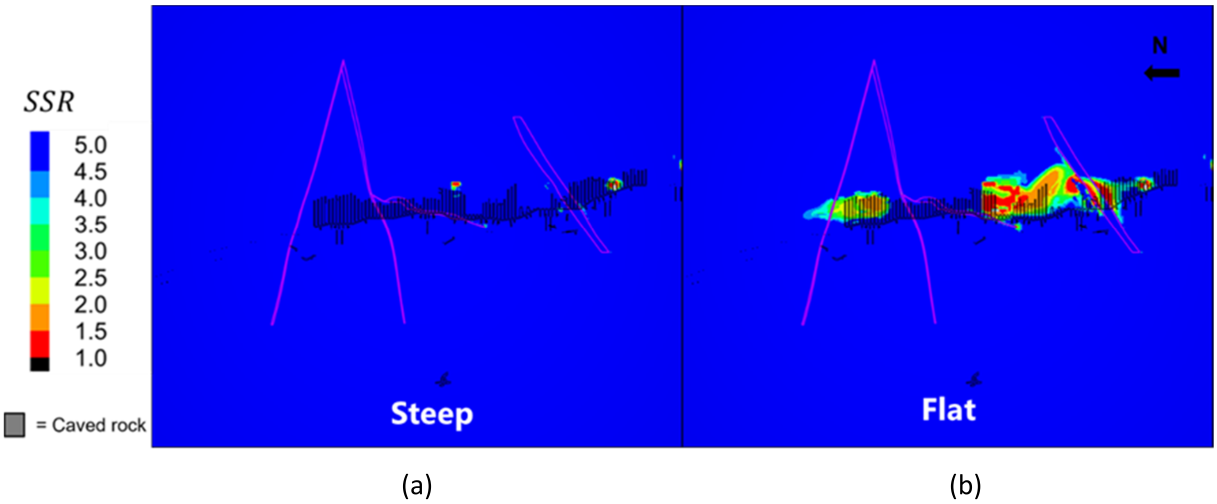


**Figure 7 Strength-stress ratio in (a) a steep and (b) a flat chevron sequence before opening a new mining level at 1,252 m**

### *3.4.2 Number of mining fronts*

The results showed that a chevron sequence with two mining fronts (sequences A.2 and B.2) can result in significantly less slipping and shear deformations of the DB compared to the sequences with a single production front (Figure 8). This is because with a two-front chevron excavation sequence, mining starts north of the northern DB, creating an area of increased confinement between the excavation front and the south DB. The single-front mining sequences approaches the north DB from south to north, causing deconfinement of the northern DB and (Figure 9) leading to larger shear displacements and slip.

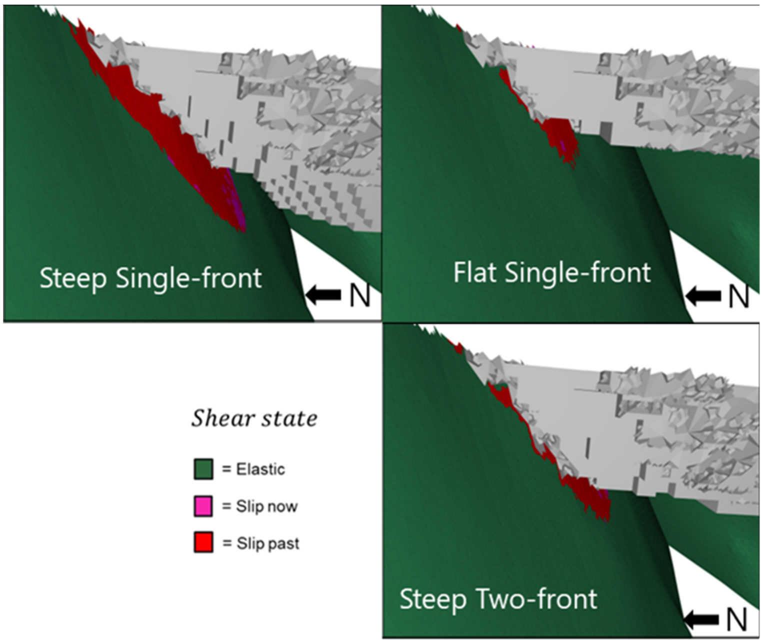


**Figure 8 Slip of the north diabase dyke when crossing it with alternative chevron sequences**

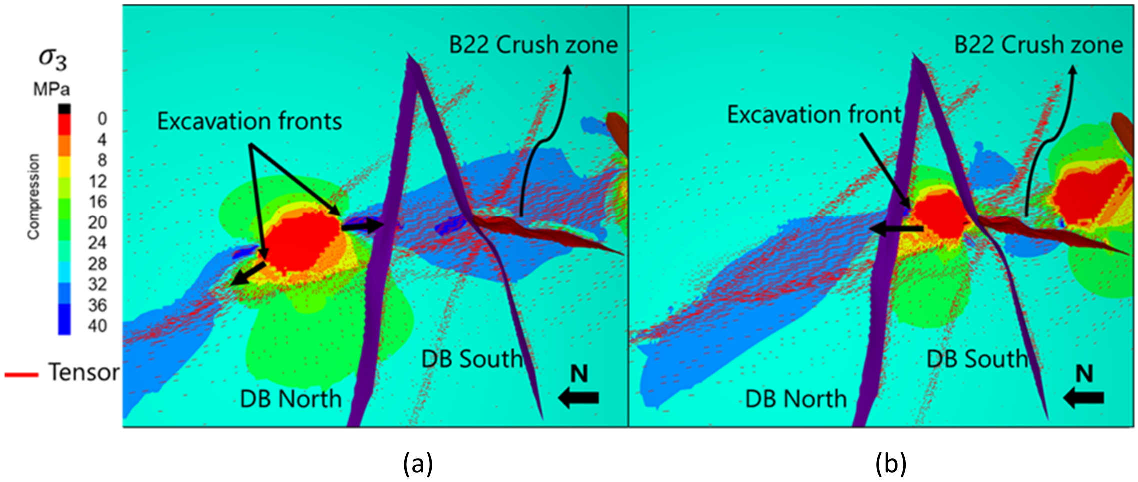


**Figure 9 Confinement of the north diabase dyke when approaching it with (a) a two-front and (b) a single-front chevron sequence**

### *3.4.3 Recommendation for continued analysis*

The results from the first stage of the numerical study showed that:

- A flat chevron sequence generally has a larger footprint on the level below the current mining level, causing stress increase on it. With a steep chevron sequence the influence from the mined-out levels above the currently mined level is limited, providing relatively better stress conditions at each mining level.
- Flat sequences are generally more beneficial than steep chevrons when crossing the DB.
- Two-front chevron sequences are the most beneficial when crossing the DB, causing the lowest shear slip and displacements due to the mining direction (north to south).

Based on these findings, a 'mild' (flatter) two-front chevron sequence was recommended for the second stage of the analysis, as described below.

# 4 Analysis with coupled flow model

## 4.1 Mining sequence

Based on the suggestion from the first stage of the analysis, a new mining sequence was developed and analysed to investigate the influence of continued mining on the main mining level located at 1,365 m. The sequence developed was a mild chevron sequence with two mining fronts on each side of the barrier pillar. Mining on the north side of the pillar is continuing below the main haulage level, following the orebody toward depth, until the main level is fully excavated. Mining on the south side of the pillar stops at the main level. The progression of the mining sequence (grey) together with some of the mining infrastructure (red) for selected years is shown in Figure 10.

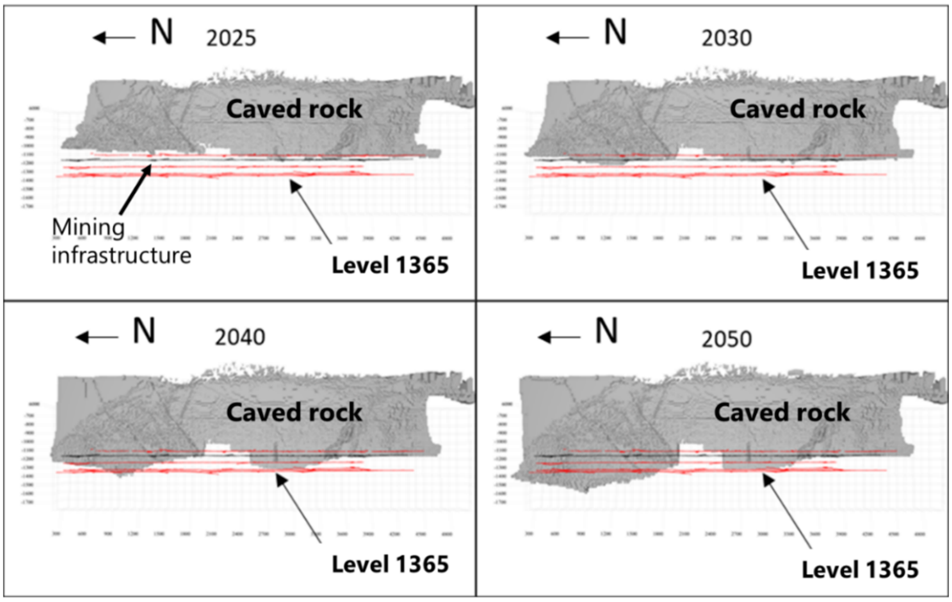


**Figure 10 Progression of the mining sequence for selected years**

The analysis was performed using a coupled MassFlow-FLAC3D model to more accurately account for the caving of the hanging wall during the mining sequence. MassFlow represents the latest development of the material flow code REBOP. REBOP was developed to emulate flow behaviour observed in explicit discontinuum PFC simulations and large-scale physical experiments, but in a much more rapid manner and at a larger scale (hence the name rapid emulator-based on PFC; REBOP) (Figure 11). A detailed description of MassFlow and the underlaying physics and formulas can be found in Itasca Consulting Group (2023b).

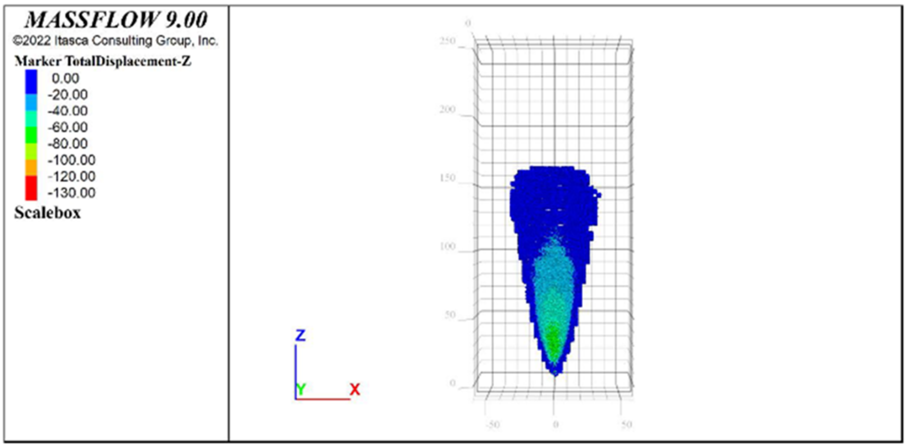


**Figure 11 Volume associated with extraction of material from an isolated drawpoint simulated in MassFlow**

## 4.2 Effect on the main haulage level (1,365 m)

The maximum tangential stress ($\sigma_\tau = 3 \times \sigma_1 - \sigma_3$) for a circular opening is used as an approximation of the induced stress around excavations. This was applied since no infrastructure is included in the model. High tangential stress values ($\sigma_\tau > 0.4 \times \mathrm{UCS}$) in strong hard rock has been associated with increased hazard for deep-seated stress-driven failures (Kaiser & Cai 2013). For evaluation of the results on the main level, 3D volumes representing parts of the elastic rock mass where the predicted theoretical tangential stress exceeds 150 MPa were used. This criterion was based on previous back-analyses of several rockfalls in Kiirunavaara Mine and has been used as an indicator for increased risk for the occurrence of seismic-related events.

The first time a portion of the north side of the 1,365 m level falls into the 'influenced zone' (regions of the rock mass for which the criterion is exceeded, i.e. red volume) is for the chute gallery located around Y = 1,100 for the simulated year 2031 (Figure 12). At this stage the chevron tip has reached the 1,252 m level and is located around Y = 1,200. As the mining front advances the influenced zone will expand north and south along the chute galleries. As the chevron tip and the rest of the chevron front moves below the 1,365 m level, a stress reduction on parts of the infrastructure located behind the cave front is observed. The chevron will, however, continually push the influenced zone north and south along it until mining has commenced along the entire level.

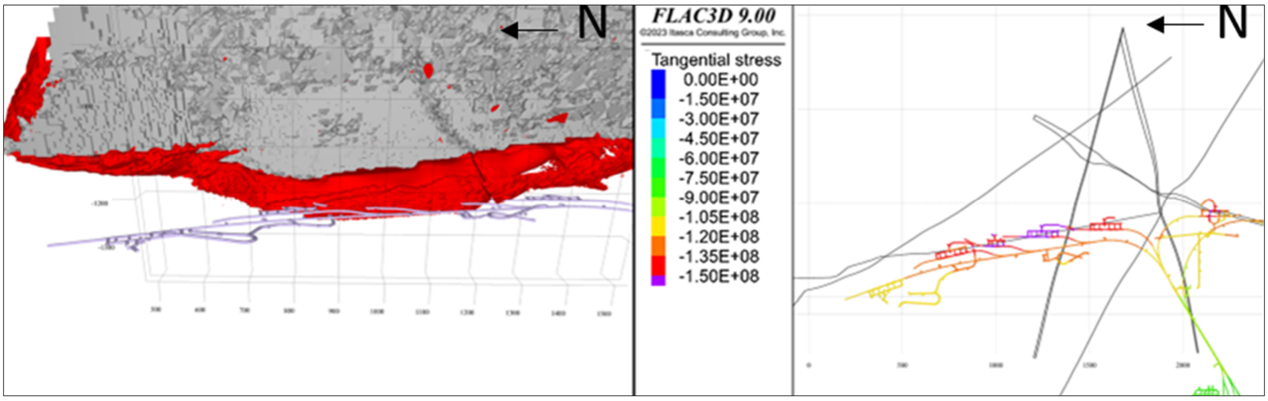


(a) (b)

**Figure 12 (a) 3D view, from the footwall side, of the area with tangential stress over 150 MPa (in red) together with caved rock (in grey), along with (b) top view of tangential stress on the infrastructure of the main level for the year 2031**

Results for the southern region indicate that the existing weakness zones (B22 crushed zone, Major dextral and Plane_1) have a major influence on the stability of the main level. According to the analysis the rock around and between these zones is very likely to attract high stress, exceeding the limit values of the previously defined criterion, and be subjected to even higher risk for stress-induced failures relative to the north side. The tangential stress criterion is first exceeded around the year 2030, and the 'affected zone' expands in the areas adjacent to the weakness zones. Since the south part of the main level will have to remain operational until at least 2063 (long after the excavation of the south part of the orebody), rehabilitation of the infrastructure is likely to be required (Figures 13 and 14).

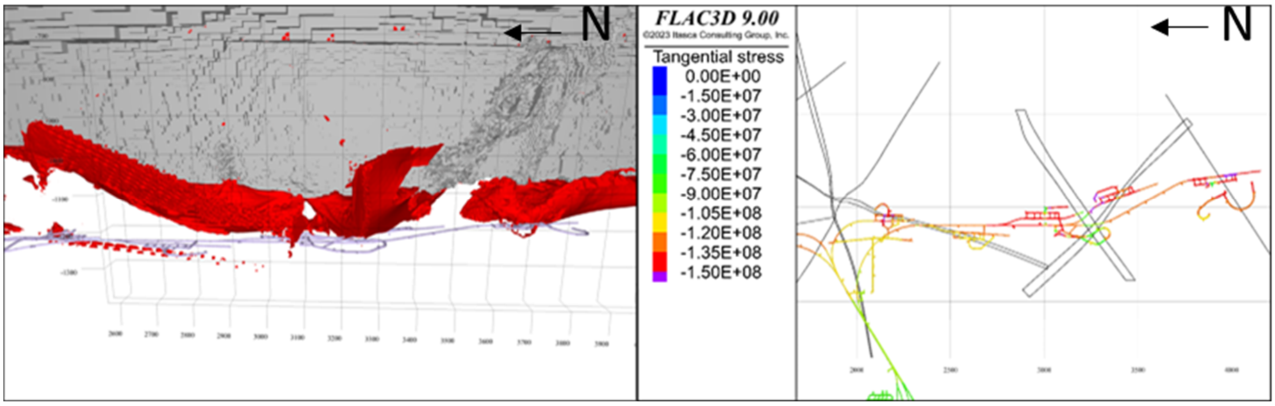


(a) (b)

**Figure 13 (a) 3D view, from the footwall side, of the area with tangential stress over 150 MPa (in red) together with caved rock (in grey), along with (b) top view predicted tangential stress on the infrastructure of the main level for the year 2031**

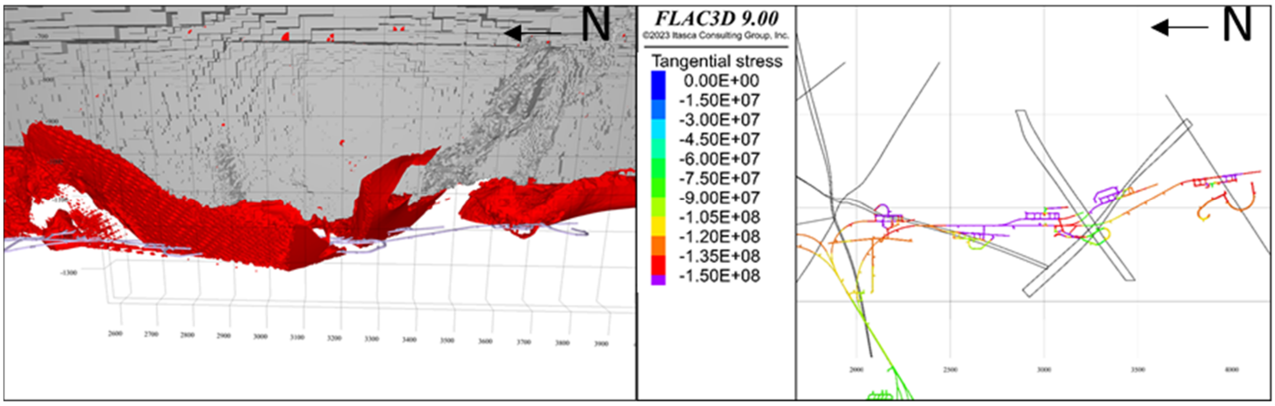


(a) (b)

**Figure 14 (a) 3D view, from the footwall side, of the area, with tangential stress over 150 MPa (in red) together with caved rock (in grey), along with (b) top view predicted tangential stress on the infrastructure of the main level for the year 2050**

## 4.3 Behaviour of large-scale structures

### *4.3.1 Diabase dykes*

The behaviour of the south and north DB is critical to mining as they have been historically associated with several large seismic events and can affect the final placement of the barrier pillar. The results from the coupled analysis show that the selected mining sequence (mild two-front chevron) has indeed been a positive influence on their behaviour, since no notable shear displacements are observed in connection with the advancing mining front and only a minor region located adjacent to the mining front is slipping (Figure 15).

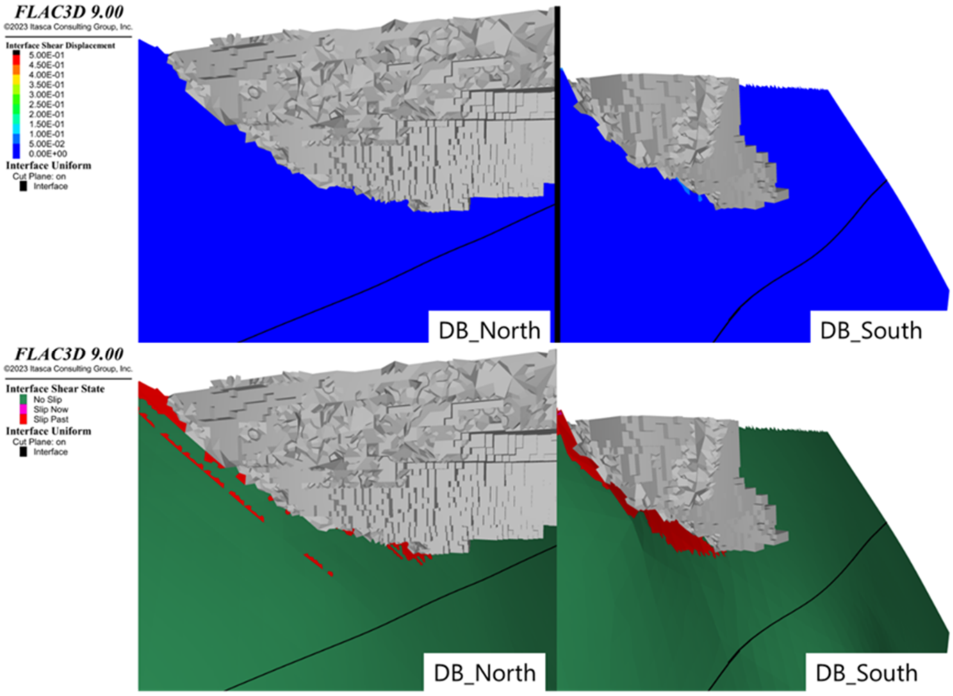


**Figure 15 Shear displacement (up) and slip (down) on the diabase dykes for the year 2045**

### *4.3.2 Plane_1*

Plane_1 is modelled as weak rock mass with a slip plane on each side of it simulating contact with the host rock. Results for the shear displacements on the slip planes of Plane_1 show that there is potential for large shear movements along the structure, mainly located below the mining front. As the chevron-shaped mining front closes in on Plane_1 and then penetrates it, there is a large increase in the shear displacements occurring in in the vicinity of the mining front (Figure 16). Given the problematic stress situation seen in the rock mass around Plane_1 (see Section 4.2) and the large shear displacement along the structure, it can be assumed that mining in the vicinity of Plane_1 will be associated with an increased hazard.

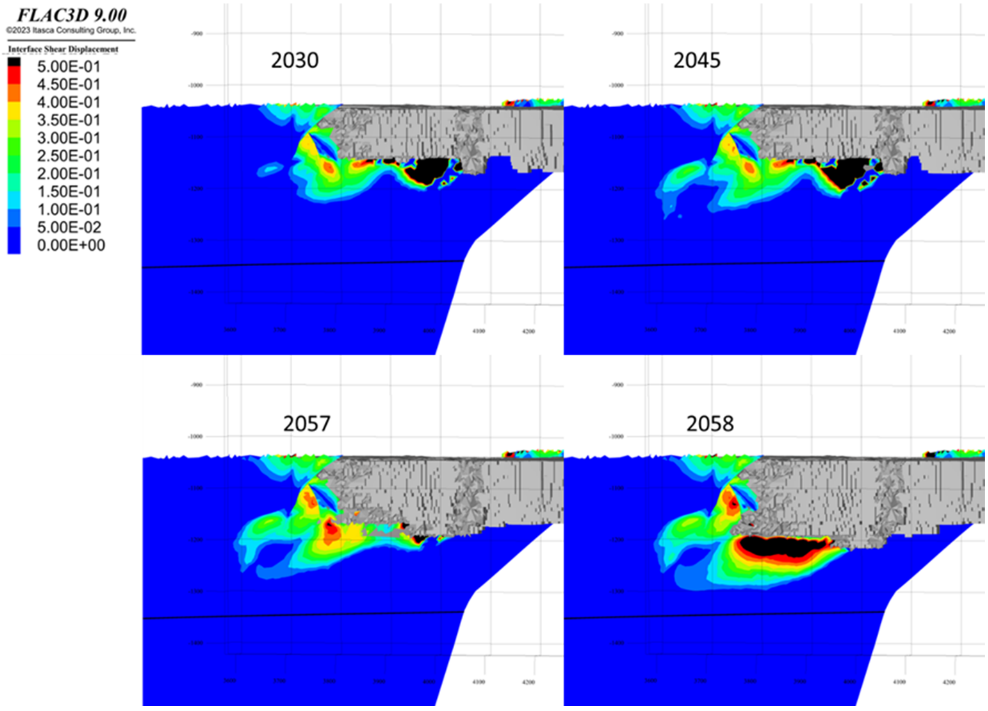


**Figure 16 Shear displacements on Plane_3**

# 5 Conclusion and recommendations

The analysis showed that a change of the currently used mining sequence to a more pronounced V-shape (chevron sequence) with a double-front can provide more favourable stress conditions during the opening of new levels but also when mining through geological structures with slipping potential. The results of the study will be taken into consideration by the mine as an input to the decision-making process for the transition to a long-term sustainable mining sequence.

The use of a chevron sequence will lead to a more rapid downward advancement compared to the earlier LOMP's with a flatter mining front. This will result in different portions of critical infrastructure located on level 1365 being affected differently, and in different time periods, depending on their location relative to the chevron tip. Additional studies are recommended for the early identification of the more critical areas and the creation of a support/rehabilitation plan. Furthermore, the advancement of the chevron tip below the 1365 level north of the pillar means that plans are needed for the transportation of the material mined below the main haulage level.

These problematic areas are indicated to occur partly in connection with the stress redistribution due to the mining sequence itself, but also, to a great extent, the existence of several main weakness zones, mostly in the south portion of the mine. The extent as well as the mechanical properties of these zones have not yet been investigated in detail. Given their significant impact on the numerical results further work is recommended to investigate their behaviour and characteristics in more detail.

# Acknowledgement

The authors thank LKAB for allowing the publication and presentation of this work.

# References

Ghazvinian, E, Garza-Cruz, T, Bouzeran, L, Fuenzalida, M, Cheng, Z, Cancino, C, Pierce, M 2020, 'Theory and Implementation of the Itasca Constitutive Model for Advanced Strain Softening (IMASS)' in R Castro, F Báez & K Suzuki (eds), *MassMin 2020: Proceedings of the Eighth international Conference and Exhibition on Mass Mining*, University of Chile, Santiago, pp. 451–461.

Itasca Consulting Group 2023a, *FLAC3D (Fast Lagrangian Analysis of Continua 3D)*, version 9.0, computer software, Minneapolis.

Itasca Consulting Group 2023b, *MassFlow*, version 9.0, computer software, Minneapolis.

Kaiser, PK & Cai, M 2013, 'Critical review of design principles for rock support in burst-prone ground - time to rethink!', in Y Potvin & B Brady (eds), *Ground Support 2013: Proceedings of the Seventh International Symposium on Ground Support in Mining and Underground Construction*, Australian Centre for Geomechanics, Perth, pp. 3–37, https://doi.org/10.36487/ACG_rep/1304_01_Kaiser

Malmgren, L & Nordlund, E 2008, 'Interaction of shotcrete with rock and rock bolts—a numerical study', *International Journal of Rock Mechanics & Mining Sciences*, vol. 45, pp. 538–553.

Sandström, D 2003, *Analysis of the Virgin State of Stress at the Kiirunavaara Mine*, Licentiate thesis, Luleå University of Technology, Sweden, Luleå.

Svartsjaern, M, Rentzelos, T, Shekhar, G, Swedberg, E, Boskovic, M & Hebert, Y 2022, 'Controlled reopening of the Kiirunavaara production block 22 after a 4.2 magnitude event', in Y Potvin (ed.), *Caving 2022: Proceedings of the Fifth International Conference on Block and Sublevel Caving*, Australian Centre for Geomechanics, Perth, pp. 685–698, https://doi.org/10.36487/ACG_repo/2205_47

Svartsjaern, M, Andersson, J, Rentzelos, T, Sekhar, G, Boskovic, M, Swedberg, E, Töyrä, J 2023, 'Options for continued mining in Kiirunavaara mine', *Proceedings of Bergdagarna 2023*, Swedish Rock Engineering and Rock Mechanics Associations, Stockholm.

Villegas, T & Nordlund, E 2008, 'Numerical Analysis of the Hanging wall Failure at the Kiirunavaara Mine', *Proceedings of MassMin 2008*, Luleå University of Technology, Luleå, pp. 867–876.